Development 130, 1069-1078

doi:10.1242/dev.00337

Targeted deletion of a branchial arch-specific enhancer reveals a role of *dHAND* in craniofacial development

Hiromi Yanagisawa[1], David E. Clouthier[2], James A. Richardson[1,3], Jeroen Charité[1,*] and Eric N. Olson[1,†]

Departments of [1]Molecular Biology, [3]Pathology, University of Texas Southwestern Medical Center at Dallas, TX 75390-9148, USA
[2]Department of Molecular, Cellular and Craniofacial Biology, Birth Defects Center, School of Dentistry, University of Louisville, Louisville, KY 40292, USA
*Present address: Department of Cell Biology and Genetics, Erasmus Medical Center Rotterdam, Dr Molewaterplein 50, 3015GE Rotterdam, The Netherlands
[†]Author for correspondence (e-mail: eolson@hamon.swmed.edu)

Accepted 12 December 2002

SUMMARY

The basic helix-loop-helix transcription factor dHAND is expressed in the mesenchyme of branchial arches and the developing heart. Mice homozygous for a *dHAND* (*Hand2*) null mutation die early in embryogenesis from cardiac abnormalities, precluding analysis of the potential role of *dHAND* in branchial arch development. Two independent enhancers control expression of *dHAND* in the heart and branchial arches. Endothelin-1 (ET-1) signaling regulates the branchial arch enhancer and is required for *dHAND* expression in the branchial arches. To determine the potential role of *dHAND* in branchial arch development and to assess the role of the ET-1-dependent enhancer in *dHAND* regulation in vivo, we deleted this enhancer by homologous recombination. Mice lacking the *dHAND* branchial arch enhancer died perinatally and exhibited a spectrum of craniofacial defects that included cleft palate, mandibular hypoplasia and cartilage malformations. Expression of *dHAND* was abolished in the ventolateral regions of the first and second branchial arches in these mutant mice, but expression was retained in a ventral domain where the related transcription factor eHAND is expressed. We conclude that *dHAND* plays an essential role in patterning and development of skeletal elements derived from the first and second branchial arches and that there are heterogeneous populations of cells in the branchial arches that rely on different cis-regulatory elements for activation of *dHAND* transcription.

Key words: dHand, Craniofacial development, Neural crest, Cleft palate

INTRODUCTION

Craniofacial development involves a complex series of morphogenetic and molecular events in which diverse cell types within the branchial arches give rise to bones, cartilage and nerves of the head and neck (Noden, 1988). Neural crest cells, which originate from the dorsal lip of the neural tube, migrate into the developing branchial arches and execute specialized programs of migration, patterning, proliferation and differentiation in response to extracellular signals and interactions with adjacent epithelial and mesodermal cells (Le Douarin, 1982; Lumsden et al., 1991; Maschhoff and Baldwin, 2000; Trainor et al., 2002). This unique population of cells serves as the source of precursors for the craniofacial skeleton, as well as a subset of peripheral neurons and vascular structures. While it is apparent that neural crest cell diversification is essential for the genesis of these different craniofacial structures, relatively little is known of the transcriptional pathways that subdivide populations of neural crest cells in different territories within the developing branchial arches.

The peptide ligand endothelin-1 (ET-1; also known as Edn1) plays a key role in regulating branchial arch development. Targeted mutations of the genes encoding ET-1, the G protein-coupled endothelin receptor A (ETA, EndrA) and endothelin converting enzyme-1 (ECE-1), show identical phenotypes characterized by abnormalities in branchial arch-derived skeletal elements, arteries and the cardiac outflow tract (Clouthier et al., 1998; Kurihara et al., 1995; Kurihara et al., 1994; Yanagisawa et al., 1998). ET-1 is secreted by the surface epithelium and the paraxial mesodermal core of the branchial arches, and acts on surrounding ectomesenchymal cells that express ETA. Pharmacological interventions with an ETA antagonist in chick embryos showed that ET-1/ETA-mediated signaling is critical for development of the lower beak and other distal branchial arch derivatives during the time period corresponding to colonization of *EndrA*-positive post-migratory neural crest cells (Kempf et al., 1998). In addition, the gene responsible for the *sucker* mutation in zebrafish was shown to encode ET-1, and defects observed in *sucker* mutants, such as severe hypoplasia of the lower jaw and malformations of distal (ventral) branchial arch cartilages can be rescued by injection of ET-1 orthologs or administration of human recombinant ET-1 (Miller et al., 2000). These findings suggest

that a common signaling pathway involving ET-1/ETA is conserved between zebrafish, birds and mammals, and is essential for development of branchial arch-derived structures.

ET-1 is required for expression of the basic helix-loop-helix (bHLH) transcription factor genes *dHAND*/*Hand2* and *eHAND*/*Hand1* in the mesenchyme of the anterior branchial arches (Thomas et al., 1998; Clouthier et al., 2000). We have shown that a 208 bp enhancer upstream of the *dHAND* gene is sufficient to drive expression of *dHAND* in the mandibular component of branchial arch 1 and branchial arch 2 (hyoid arch) in mice, and that activity of this enhancer is completely abolished in *EdnrA*$^{-/-}$ null embryos, suggesting that it is a downstream target for ETA signaling (Charité et al., 2001). This enhancer contains a series of conserved ATTA motifs that correspond to the consensus-binding motif for many homeodomain proteins. Mutation of these sites abolishes expression of a linked transgene in branchial arches 1 and 2 of transgenic mouse embryos at E10.5, suggesting that binding of homeodomain transcription factors to these sites is essential for enhancer activity. Consistent with this notion, the distal-less homeodomain protein Dlx6 binds these sites and is expressed in a pattern that overlaps that of *dHAND* in the branchial arches. Expression of *Dlx6* is undetectable in the distomedial branchial arches of *EdnrA*$^{-/-}$ embryos, suggesting that Dlx6 is a key transcription factor involved in ETA-dependent regulation of *dHAND* in the branchial arch.

Because mice homozygous for a *dHAND* null allele die from cardiac abnormalities prior to branchial arch development, the specific role of *dHAND* in development of these structures has been unclear. To address this question, we generated mutant mice in which the ETA-dependent neural crest enhancer of *dHAND* was deleted by homologous recombination. Mice homozygous for this enhancer deletion fail to express *dHAND* in the ventrolateral region of the first and second branchial arches and show lethal craniofacial abnormalities that include cleft palate and malformations of the mandible and Meckel's cartilage. However, expression of *dHAND* in the ventral region of the branchial arches is retained in these mutant mice, demonstrating the involvement of additional cis-regulatory elements in the control of branchial arch expression of *dHAND*. These findings demonstrate an essential role for *dHAND* in craniofacial development and reveal unanticipated molecular heterogeneity in the transcriptional pathways that subdivide cells within the branchial arch neural crest.

MATERIALS AND METHODS

Gene targeting

Three overlapping *dHAND* phage clones encompassing approximately 18-kb of upstream flanking sequence were isolated from a mouse 129 SV genomic library using the *dHAND* cDNA as a probe (Srivastava et al., 1997), and cloned into pBluescript vector (Stratagene, Inc.) for endonuclease restriction mapping. A 754 bp *Xho*I-*Bam*HI fragment containing a 208 bp branchial arch enhancer SspBam208 described previously (Charité et al., 2001) was replaced by a *neo*^{r} gene cassette driven by the PGK promoter and floxed by two loxP sites (see Fig. 1). A 3 kb fragment 5′ to the unique *Xho*I site was used as a short arm and a ~6 kb *Bam*HI-*Not*I fragment was used as a long arm; a thymidine kinase gene driven by the MCI promoter was used for negative selection. An *Xba*I site was introduced adjacent to the 5′ end of an upstream loxP site in the targeted construct.

Linearized targeting vector DNA was electroporated into SM-1 embryonic stem (ES) cells, which were subsequently selected under G418 and FIAU as described previously (Yanagisawa et al., 2000). Genomic DNA was prepared from ES cell clones and digested with *Sac*I for hybridization with a 5′ probe, and with *Nde*I and *Xba*I for a 3′ probe. Targeted clones were expanded and injected into blastocysts from C57BL/6 mice and resultant chimeras were bred to C57BL/6 mice to obtain germ line transmission. Heterozygous mutant mice for the *dHAND* branchial arch enhancer (+*neoBAenh*) were intercrossed to obtain +*neoBAenh*$^{-/-}$ homozygous mutants. To obtain heterozygous mutants for the branchial arch enhancer without a *neo*^{r} cassette (Δneo*BAenh*), +*neoBAenh*$^{+/-}$ heterozygous mutants were bred to transgenic mice expressing Cre recombinase under the cytomegalovirus immediate early enhancer-chicken β-actin hybrid promoter (CAG) (Sakai and Miyazaki, 1997). The resulting Δ*neoBAenh*$^{+/-}$ heterozygous mutants were bred to the +*neoBAenh*$^{+/-}$ heterozygous mutants to obtain Δ*neoBAenh*$^{-/-}$ homozygous mutants.

Genotyping and PCR

Genotyping was performed by Southern blot analysis using genomic DNA isolated from tail biopsies or yolk sac preparations. We performed PCR amplifications of the *neo* gene (5′-TTCCACC-ATGATATTCGGCAAGCAGG-3′ for an upstream primer and 5′-TATTCGGCTATGACTGGGCACAACAG-3′ for a downstream primer), and the *BAenh* sequence (5′-TCTGATCTCCTTTCAAACT-3′ for an upstream primer and 5′-ATTTCCAGCAAGCATCCTGC-3′ for a downstream primer) to identify +*neoBAenh*$^{+/-}$, +*neoBAenh*$^{-/-}$ or the Δ*neoBAenh*$^{-/-}$ mutants. For detection of the Cre transgene, PCR primers (5′-AGGTTCGTTCACTCATGGA-3′ for an upstream primer and 5′-TCGACCAGTTTAGTTACCC-3′ for a downstream primer) were used. For a control, PCR primers (5′-TGGATAATACAA-TGATGTGGAAAATGGGA-3′ for an upstream primer and 5′-AGCTCCTAGCTATGGGTTCTC-3′ for a downstream primer) were used. Southern blot analysis was performed to distinguish wild-type mice from the Δ*neoBAenh*$^{+/-}$ mice.

Histology and skeletal analysis

For routine histological analysis, embryos were fixed in 10% neutral buffered formalin, embedded in paraffin and sectioned at 5 μm. Paraffin sections were stained with Hematoxylin and Eosin. For skeletal analysis, postnatal day 1(P1) embryos were collected, prepared and stained with Alizarin Red and Alcian Blue to examine bone and cartilage formation, respectively (Yanagisawa et al., 1998). Cartilaginous fetal skeletons (E14.5) were prepared and stained with Alcian Blue as previously described (Jegalian and De Robertis, 1992).

In situ hybridizations

E10.5 embryos were harvested and fixed in 4% paraformaldehyde overnight at 4°C. Riboprobes for *dHAND*, *eHAND* and *Dlx6* were prepared as described previously (Charité et al., 2001; Thomas et al., 1998) with ^{35}S-UTP (Amersham) using the Maxiscript In Vitro Translation Kit (Ambion). In situ hybridizations were performed as described previously (Shelton et al., 2000).

Whole-mount in situ hybridization

Embryos were harvested at E10.5 and fixed in 4% paraformaldehyde overnight at 4°C. Whole-mount in situ hybridizations were performed as previously described (Clouthier et al., 2000) using digoxigenin-labeled riboprobes for *dHAND*, *eHAND*, *MHox*, *Msx1* and *Msx2* (Thomas et al., 1998), *Gsc*, *Dlx2* and *Dlx3* (Clouthier et al., 2000), *Dlx5* [a gift from J. L. R. Rubenstein (Liu et al., 1997)] and *Dlx6* (a gift from G. Levi) and Alx3 (ten Berge et al., 1998). At least 3 embryos per genotype were examined per probe. Following whole-mount in situ hybridization, embryos were photographed using an Olympus SZX12 photomicroscope with an attached DP11 digital camera.

RESULTS

Targeted disruption of a *dHAND* branchial arch enhancer

We have previously identified an evolutionarily conserved 208 bp enhancer that directs *dHAND* expression in the first and second branchial arches during mouse embryogenesis (Charité et al., 2001). To test whether this enhancer is required for *dHAND* expression in vivo, and to further clarify the role of *dHAND* in development of branchial arch-derived structures, we generated a mutant *dHAND* gene in which a 754 bp *Xho*I-*Bam*HI fragment containing the branchial arch enhancer was deleted by homologous recombination. The deleted 754 bp region was replaced with a *neo*^{r} cassette driven by the PGK promoter (+*neoBAenh*). In order to avoid possible interference of the PGK promoter with *dHAND* expression, we flanked the *neo*^{r} cassette with two loxP sites to permit removal of the *neo*^{r} cassette by Cre-recombinase, yielding a mutant gene referred to as Δ *neoBAenh*. This strategy has been used in other enhancer deletion studies in mice (Bouvier et al., 1996; Danielian et al., 1997).

The targeting vector was electroporated into ES cells and 480 colonies were screened by Southern blot analysis. Four independent ES clones containing a +*neoBAenh* mutant allele (data not shown) were injected into blastocysts obtained from C57BL/6 mice, and 6 chimeras were obtained. Three chimeras from two independent ES cell clones transmitted the mutant allele through the germline. The +*neoBAenh* heterozygous mice were then bred to transgenic mice expressing Cre-recombinase under control of the CAG promoter to establish heterozygous mutant mice carrying the Δ *neoBAenh* mutant allele in the germline. Despite reported activity of the CAG promoter in female oocytes (Sakai and Miyazaki, 1997), Cre recombinase-mediated loxP deletion was not observed without integration of the transgene in the genome, suggesting that recombination did not occur in the germ cells of +*neoBAenh*$^{+/-}$ mice (data not shown).

The +*neoBAenh*$^{+/-}$ mice carrying the Cre transgene were bred to +*neoBAenh*$^{+/-}$heterozygous mutant mice, and genotyping of progeny was performed by Southern blot analysis. As shown in Fig. 1B, hybridization of *Sac*I-digested tail DNA with a 5′ probe resulted in a 13.5 kb band for the wild-type and Δ *neoBAenh* alleles, whereas the +*neoBAenh* allele gave a 6.5 kb band because of an additional *Sac*I site in the *neo*^{r} cassette. Hybridization of *Nde*I- and *Xba*I-digested tail DNA with a 3′ probe yielded bands of 16 kb for the wild-type allele, 12 kb for the +*neoBAenh* allele and 9.5 kb for the Δ *neoBAenh* allele. Next, we performed PCR analyses to confirm that the branchial arch enhancer sequence was deleted in +*neoBAenh*$^{-/-}$ and Δ *neoBAenh*$^{-/-}$ mice. As shown in Fig. 1C, a 500 bp *neo* band was absent in the presence of Cre-recombinase and a 300 bp band corresponding to the branchial arch enhancer was absent both in the +*neoBAenh*$^{-/-}$ and the Δ *neoBAenh*$^{-/-}$ mutants.

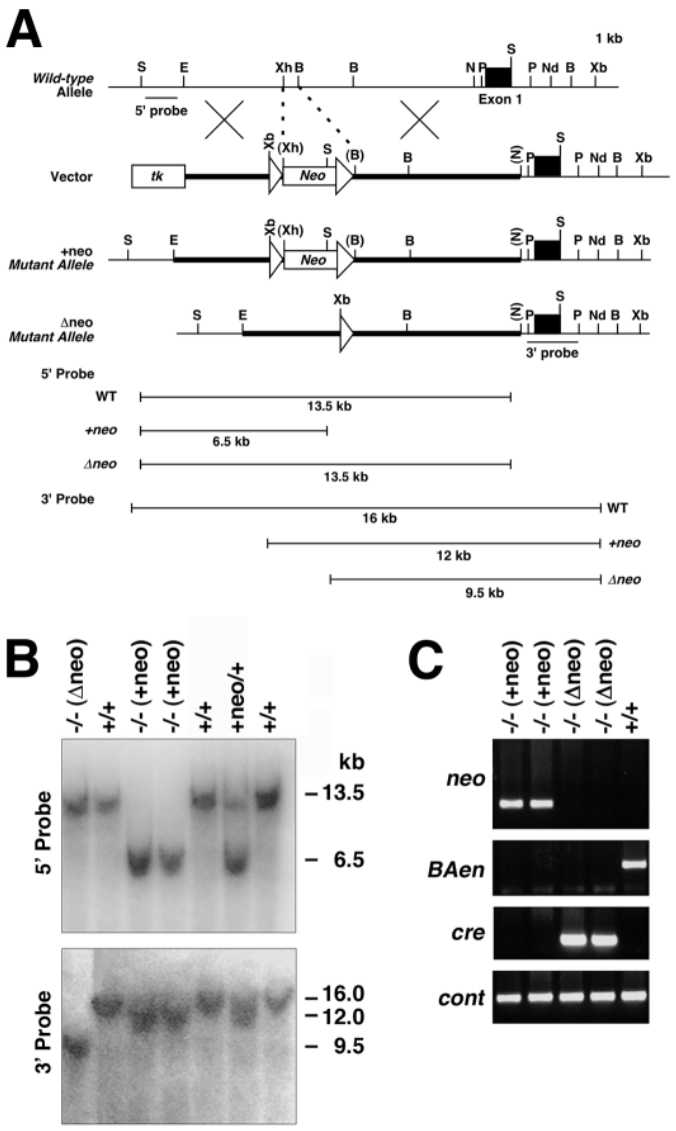

Fig. 1. Generation of *BAenh*$^{-/-}$ mice. (A) Targeting strategy. A 754 bp *Xho*I-*Bam*HI fragment containing a 208 bp branchial arch-specific enhancer was replaced with a *neo*^{r} cassette flanked by loxP sites (triangles), introducing an *Xba*I site at the 5′ end of the cassette. The +*neoBAenh* mutant allele contains a *neo*^{r} cassette. Cre-mediated recombination of this allele generated the Δ*neoBAenh* mutant allele. tk, thymidine kinase; S, *Sac*I; E, *Eco*RI; Xh, *Xho*I; B, *Bam*HI; N, *Not*I; Nd, *Nde*I; P, *Pst*I; Xb, *Xba*I. (B) Southern blot analysis of tail DNA digested with *Sac*I and hybridized with a 5′ probe (upper panel), or digested with *Nde*I and *Xba*I and hybridized with a 3′ probe (lower panel). The genotype is listed on the top of each lane. (C) PCR genotype of tail DNA. Each panel shows a PCR reaction amplifying a 500 bp *neomycin* gene (neo), a 300 bp fragment containing the branchial arch enhancer of *dHAND* (BAen), a 300 bp Cre-recombinase fragment (cre) and a 302 bp control sequence (cont).

Deletion of the branchial arch enhancer is sufficient to cause craniofacial abnormalities in *BAenh*$^{-/-}$ embryos

Genotyping of postnatal day 28 mice revealed no viable *BAenh*$^{-/-}$ mice among more than 100 offspring examined. The *BAenh*$^{-/-}$ mutants with or without a *neo*^{r} cassette showed an identical phenotype of hypoplastic jaw (Fig. 2A), and all died within 24 hours of birth from failure to suckle. The secondary palate of the mutants failed to fuse along the midline of the oral shelf (Fig. 2B), and the stomach contained no milk. In the homozygous mutants there were no other gross

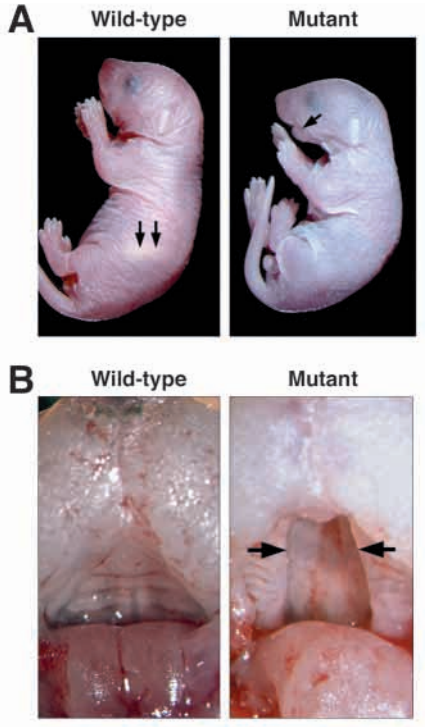

Fig. 2. Gross abnormalities of *BAenh*$^{-/-}$ mice. (A) Gross appearance of wild-type and *BAenh*$^{-/-}$ mutant mice at P1. The *BAenh*$^{-/-}$ mouse has a hypoplastic jaw (arrow) and an empty stomach. The wild-type littermate shows milk in the stomach (double arrows). (B) View of the palate of wild-type and *BAenh*$^{-/-}$ mutant mice at P1. The cleft palate in the mutant is indicated by arrows.

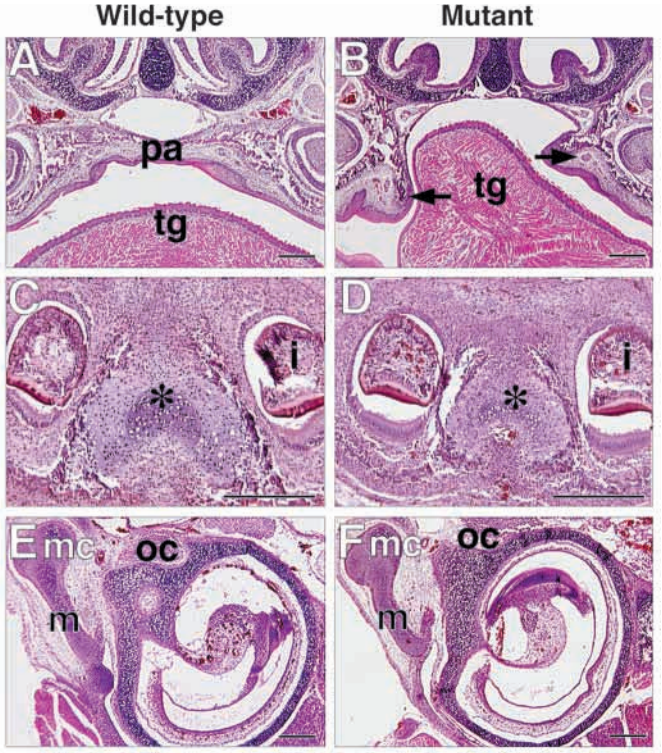

Fig. 3. Histology of wild-type (A,C,E) and *BAenh*$^{-/-}$ mutant (B,D,F) mice at P1. (A,B) The secondary palate formed by fusion of bilateral palatine bones (pa) in the wild-type mouse (A) is absent in the *BAenh*$^{-/-}$ mutant mouse (arrows in B). Muscle fibers of the tongue (tg) are irregular and sparse in the mutant mouse. (C,D) Wild-type and homozygous mutant mice both show symphysis of Meckel's cartilage (asterisk) and lower incisors (i). (E,F) The junction between the malleus (m) and Meckel's cartilage (mc) is observed in wild-type and mutant mice. oc, otic capsule. Bars indicate 300 μm.

abnormalities related to branchial arch-derived craniofacial structures, the cardiac outflow tract or the great vessels (data not shown).

Histological examinations of P1 *BAenh*$^{-/-}$ mutants showed that the mandibular bones were hypoplastic and displaced laterally compared to those of wild-type mice (data not shown). The palatine processes were elevated and fused to form the secondary palate in wild-type mice (Fig. 3A). In contrast, the secondary palate was defective in *BAenh*$^{-/-}$ mice (Fig. 3B, arrows). Consequently, the mutants had a cleft palate. The muscle fibers of the tongue were also less organized and seemed to be oriented randomly in the *BAenh*$^{-/-}$ mutant compared to wild-type littermates (tg in Fig. 3A,B). The distal symphysis of Meckel's cartilage was present in both the wild-type and the *BAenh*$^{-/-}$ mutant mice (asterisk in Fig. 3C,D), although it was smaller in the *BAenh*$^{-/-}$ mutant (Fig. 3D). Meckel's cartilage was continuously fused to the malleus at the proximal end in both wild-type and *BAenh*$^{-/-}$ mutant mice (Fig. 3E,F). Inner ear structures and middle ear ossicles were all present in the *BAenh*$^{-/-}$ mutants.

To further examine craniofacial structures in *BAenh*$^{-/-}$ mutants, we compared bone and cartilage staining of homozygous mutants with wild-type littermates at P1. We observed that the mandible of homozygous mutants was much smaller in size and shortened (ma in Fig. 4B,D), compared with the mandible in wild-type mice (ma in Fig. 4A,C). A ventral view of the skull showed deformity of the mandible in the homozygous mutant (Fig. 4D compare with C). The well-developed Meckel's cartilage was observed extending from the malleus to the middle of the mandible in the wild-type mouse (arrows in Fig. 4C). However in the *BAenh*$^{-/-}$ mutant mouse, Meckel's cartilage was disrupted at the proximal end closer to the junction to the malleus (arrow in Fig. 4D, mc in 4P). Close examination showed that the angle between the right and left mandibular bones was wider in the *BAenh*$^{-/-}$ mutant than in the wild-type mouse (Fig. 4K,L). In addition, the angular process was severely reduced, and an ectopic process was observed extending from the ventral surfaces of the mandible (Fig. 4M,N). Defects in the mandible were already apparent in *BAenh*$^{-/-}$ mutant embryos at E14.5 (Fig. 5B,D). Cartilage staining at E14.5 revealed the well-developed Meckel's cartilage in wild-type embryos (Fig. 5A). In contrast, Meckel's cartilage was obviously truncated in *BAenh*$^{-/-}$ mutant embryos (Fig. 5B). Interestingly, there was a cartilage primordium in the distal part of the mandible both in the wild-type and the *BAenh*$^{-/-}$ mutants (Fig. 5C, arrow in D). Meckel's cartilage normally forms from proximal and distal primordia, and failure of expansion from either primordium could result in a truncated Meckel's cartilage.

In P1 embryos, the tympanic rings were shortened and deformed in the *BAenh*$^{-/-}$ mutant mouse (compare arrows in Fig. 4E and F). In the wild-type mouse, bilateral palatine

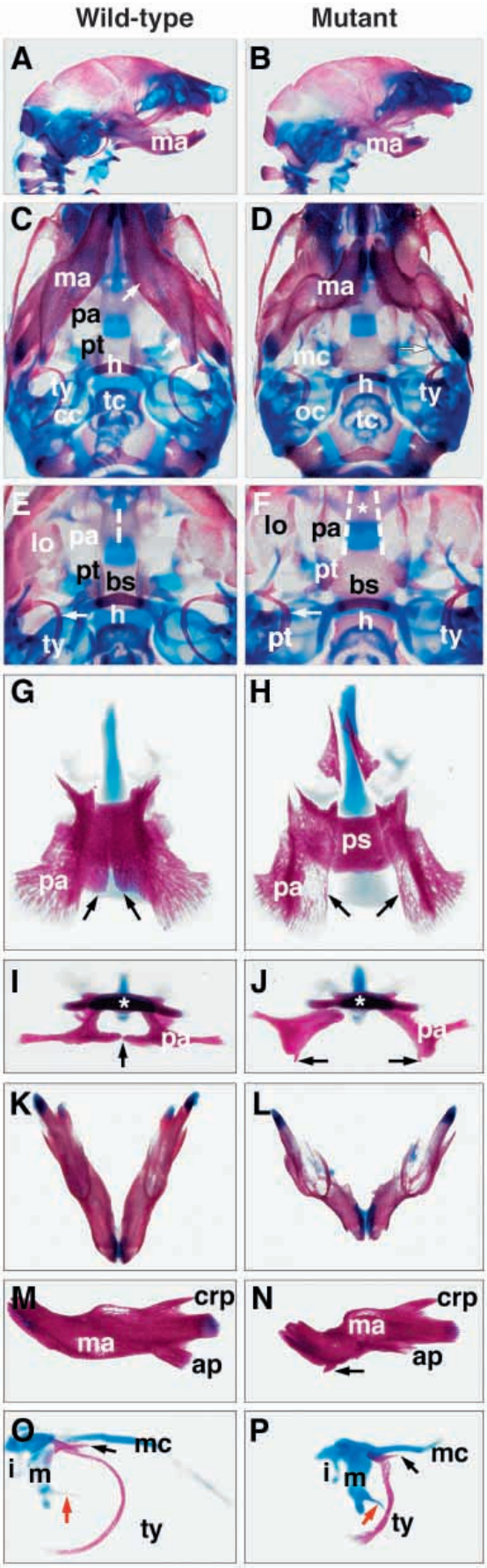

Fig. 4. Craniofacial analysis of wild-type and *BAenh*$^{-/-}$ mice at P1. (A,C,E,G,I,K,M,O) wild-type; (B,D,F,H,J,L,N,P) *BAenh*$^{-/-}$ mutant mice. (A,B) Lateral view, (C-F) ventral view, (G-P) isolated bones and cartilages. (A-D) The mandible (ma) is hypoplastic and deformed, and Meckel's cartilage (arrows in C and D) is truncated in the mutant mouse (B,D). (E,F) Tympanic rings (ty) are thickened and deformed in the mutant mouse (F, compare arrows in E and F). Fusion of the bilateral palatine processes observed in the wild type mouse (E, dashed line) is absent in the mutant mouse (F, dashed lines). Asterisk in F indicates the presphenoid bone. (G,H) In the wild-type mouse, the secondary palate is formed by the fusion of bilateral palatine processes (arrows). In the *BAenh*$^{-/-}$ mouse, the palatine processes are not formed so that the presphenoid (ps) becomes visible. (I,J) Palatine bones viewed end on. Compare black arrows in I and J, which indicate fused palatine processes and absence of palatine processes, respectively. An asterisk indicates the presphenoid bone. (K,L) Ventral views of the mandibles. Note that the mandible in the *BAenh*$^{-/-}$ mouse is shorter and deformed. The angle between the left and right mandible is wider than that in the wild-type mouse. (M,N) Lateral views of the mandibles. Note that the articular process (ap) in the *BAenh*$^{-/-}$ mouse is severely hypoplastic and an ectopic process (black arrow) is formed. (O,P) Lateral views of middle ear cartilages and tympanic ring. In the mutant mouse, Meckel's cartilage (mc) is truncated, and the tympanic ring (ty) is shortened and thickened. Black and red arrows indicate the gonial bone and manubrium of the malleus, respectively. Note that the gonial bone is hypoplastic and the projection of the manubrium is abnormal in the *BAenh*$^{-/-}$ mutant. bs, basisphenoid; crp, coronoid process; h, hyoid; I, incus; lo, lamina obturans; m, malleus; mc, Meckel's cartilage; oc, otic capsule; pa, palatine; pt, pterygoid; tc, thyroid cartilage.

processes extended horizontally and fused to form the secondary palate (dotted line in Fig. 4E, arrows in G). In contrast, the palatine processes of the *BAenh*$^{-/-}$ mouse appeared not to be elevated and thus the secondary palate was not formed (dotted line in Fig. 4F, arrows in H). This causes the underlying presphenoid bone to be visible in ventral view (ps in Fig. 4H). The pterygoid bones were also deformed so that the relative angle to the basisphenoid bone was abnormal in the *BAenh*$^{-/-}$ mutant mouse (Fig. 4F). Although the remnants of the palatine processes were detectable in the *BAenh*$^{-/-}$ mutant mouse by close examination (arrows in Fig. 4J), they did not fuse along the midline unlike those of the wild-type mouse (arrows in Fig. 4I). The middle ear ossicles seemed to be less affected, however, the projection of the manubrium of the malleus was abnormal (red arrow in Fig. 4P). Skeletal structures affected in the mutant are summarized in Table 1.

Table 1. Defects in branchial arch-derived structures in P1 *BAenh*$^{-/-}$ mutants

Arch	Structure	Abnormality
One	Mandible	Shortened
	Meckel's cartilage	Truncated
	Tympanic ring bones	Shortened and thickened
	Gonial	Mild hypoplasia
	Malleus	Abnormal projection of the manubrium
	Pterygoid bones	Failure of medial pterygoid elevation
	Palatine bones	Failure of palatal shelf elevation and fusion (cleft)
Two	Lesser horns of the hyoid	Lateral projection

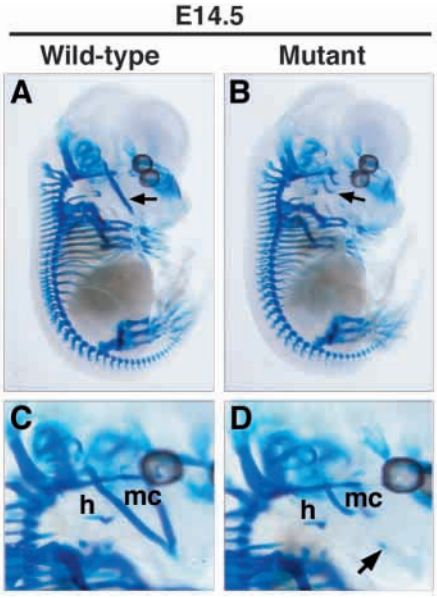

Fig. 5. Cartilage preparations of wild-type and *BAenh*$^{-/-}$ mutant embryos at E14.5. (A,C) Wild-type; (B,D) *BAenh*$^{-/-}$ mutant. In the mutant embryo, Meckel's cartilage is truncated (compare black arrows in A and B). Close examination shows that the distal primordium of Meckel's cartilage is formed in the mutant embryo (arrow in D). h, hyoid; mc, Meckel's cartilage.

dHAND expression in the ventral (distal) region of branchial arches 1 and 2 is unaffected in *BAenh* null embryos

To examine the effect of deletion of the branchial arch enhancer on *dHAND* expression, we compared *dHAND* expression in the +*neo BAenh*$^{-/-}$ and the Δ *neoBAenh*$^{-/-}$ mutants and wild-type embryos by in situ hybridization. As shown in Fig. 6, *dHAND* expression in wild-type embryos was observed in the ventral portions of the first and second branchial arches at E10.5 (Fig. 6A). In contrast, *dHAND* expression was abolished in all except the most ventral regions of branchial arch 1 in the +*neo BAenh*$^{-/-}$ (Fig. 6B,E) and the Δ *neoBAenh*$^{-/-}$ mutants (Fig. 6C). As expected, *dHAND* expression in the heart and limb was unaffected by deletion of the branchial arch enhancer (Fig. 6E).

We also examined whether *eHAND* expression was attenuated in the absence of the *dHAND* branchial arch enhancer. At E10.5, *eHAND* is expressed in the most ventral portions of branchial arches 1 and 2 of wild-type embryos (Fig. 6F). The *eHAND* expression pattern appeared identical in the branchial arches of *BAenh*$^{-/-}$ embryos (Fig. 6G and Fig. 7B), suggesting that a loss of *dHAND* expression did not induce compensatory up-regulation of *eHAND* expression. Notably, *eHAND* was not expressed in the region of the branchial arches where the *dHAND* neural crest enhancer is active. Since there is evidence for functional redundancy of *dHAND* and *eHAND* in some cell types (McFadden et al., 2002), their nonoverlapping expression in this region may account for the craniofacial phenotype in *BAenh*$^{-/-}$ embryos.

Dlx6 expression is unaffected in *BAenh*$^{-/-}$ embryos

Our previous studies showed that Dlx6 is an ETA-dependent

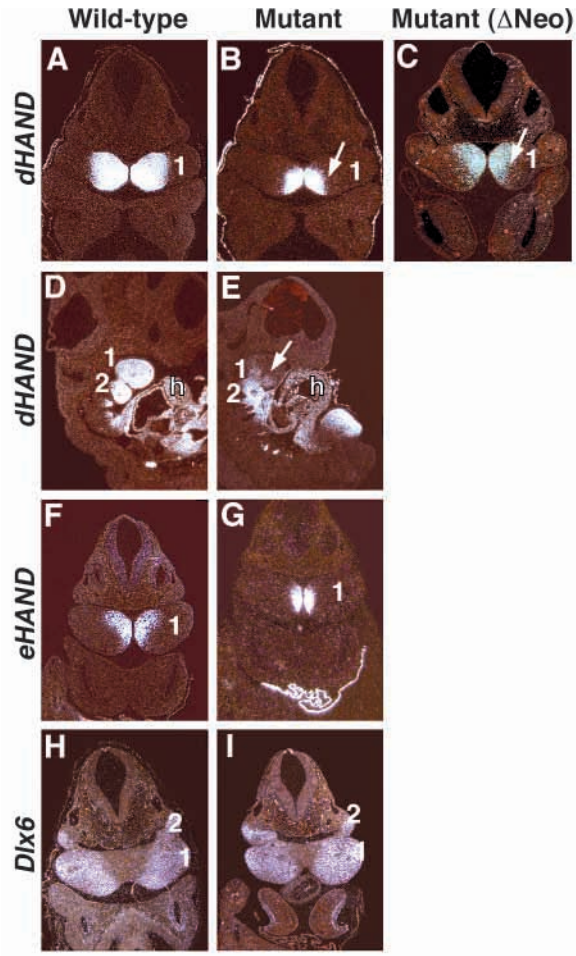

Fig. 6. In situ hybridization analysis of *dHAND*, *eHAND* and *Dlx6* transcripts in wild-type (A,D,F,H), +*neoBAenh*$^{-/-}$ (B,E,G,I) and Δneo*BAenh*$^{-/-}$ (C) embryos at E10.5. *dHAND* (A,B,C,D,E), *eHAND* (F,G) and *Dlx6* (H,I) transcripts were detected by in situ hybridization to transverse (A-C,F-H) or sagittal (D,E) sections. Note that ventrolateral *dHAND* expression in the first branchial arch of mutant embryos was absent (arrows in B,C,E), whereas heart expression was not affected (h in E). Branchial arches 1 and 2 are indicated.

branchial arch enhancer-binding factor and that the Dlx6 binding sites are essential for activity of this *dHAND* enhancer (Charité et al., 2001). To test whether Dlx6 is regulated independently of *dHAND* in the branchial arches, we examined *Dlx6* expression in *BAenh*$^{-/-}$ embryos. At E10.5, *Dlx6* expression was observed in the ventral aspect of branchial arches 1 and 2 of wild-type embryos, excluding the most ventral portions (Fig. 6H, Fig. 7G). This expression pattern was maintained in the branchial arches of *BAenh*$^{-/-}$ embryos (Fig. 6I, Fig. 7G). Most importantly, ventrolateral expression of *Dlx6*, which was down-regulated in *EdnrA*$^{-/-}$ mutant embryos, was unaffected in *BAenh*$^{-/-}$ embryos. It is interesting that *Dlx6* expression was not observed in the most ventral portion of branchial arches 1 and 2 of wild-type or *BAenh*$^{-/-}$ embryos, where *dHAND* expression persisted in *BAenh*$^{-/-}$ embryos. This suggests that transcription factor(s) other than Dlx6 may control *dHAND* expression in this region of the branchial arches.

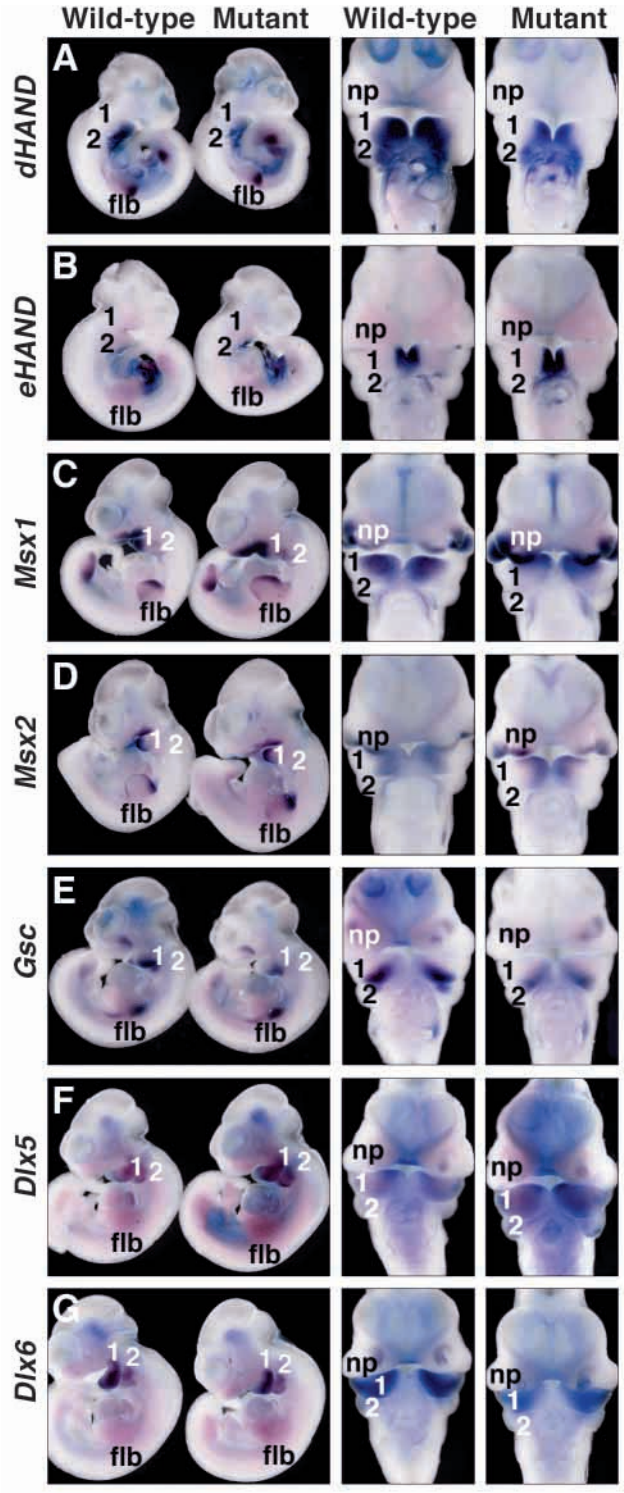

Fig. 7. Whole-mount in situ hybridization analysis of wild-type and the *BAenh*$^{-/-}$ embryos at E10.5. Left panel, lateral views; right panels, frontal views. Transcripts for *dHAND* (A), *eHAND* (B), *Msx1* (C), *Msx2* (D), *Gsc* (E), *Dlx5* (F) and *Dlx6* (G) were detected by whole-mount in situ hybridization to wild-type and *BAenh*$^{-/-}$ mutant embryos, as indicated. flb, forelimb bud; np, nasal process. Branchial arches 1 and 2 are indicated.

Effect of the *dHAND* branchial arch enhancer on expression of other transcription factors in the branchial arches

Several transcription factors, including Gsc, Dlx2 and Dlx3, are down-regulated or absent in ectomesenchymal cells of branchial arches in *EndrA*$^{-/-}$ embryos (Clouthier et al., 2000). In addition, activity of the 208 bp *dHAND* branchial arch enhancer is entirely dependent on ETA-mediated signals (Charité et al., 2001). To determine whether these factors are dependent on dHAND, we examined their expression in *BAenh*$^{-/-}$ mutants by whole-mount in situ hybridization. We chose panels of transcription factors whose expression patterns in the branchial arches overlapped spatially or temporally with that of *dHAND*, and/or that depend on ET-1/ETA mediated signals. We first examined *dHAND* expression in *BAenh*$^{-/-}$ mutants, and confirmed that *dHAND* was absent in the ventrolateral portions of the first and second branchial arches, while *eHAND* expression was not affected in the mutant embryos (Fig. 7A,B).

Msx1 and Msx2 are homeobox transcription factors regarded as general repressors of transcription in developing branchial arches, and are required for normal growth and development of branchial arch-derived structures (Satokata et al., 2000; Satokata and Maas, 1994; Takahashi et al., 2001). Msx1 was previously reported to be down-regulated in branchial arches of *dHAND* null embryos in an ET-1-independent manner (Thomas et al., 1998). The expression domains of *Msx1* and *Msx2* are overlapping and are detected in the ventrolateral aspects of the maxillary and mandibular arches of wild-type embryos at E10.5 (Fig. 7C,D). Surprisingly, *Msx1* was not down-regulated in the branchial arches of the *BAenh*$^{-/-}$ mutants. Most likely, the residual expression of *dHAND* in the ventral portion of branchial arches 1 and 2 is sufficient to induce expression of *Msx1* in the anterior branchial arches. *Msx2* expression was largely unchanged in branchial arch 1 of *BAenh*$^{-/-}$ mutants, except that the expression domain appeared to be shifted slightly ventrally (Fig. 7D, ventral view).

As we previously reported, Gsc is expressed in the ventral aspect of the posterior half of the first mandibular arch and the anterior half of the second arch at E10.5, and is severely down-regulated in *EdnrA*$^{-/-}$ embryos (Clouthier et al., 1998). Inactivation of *Gsc* in mice results in defects of most of the facial region, suggesting its role in epithelial-mesenchymal interactions (Yamada et al., 1995). As Fig. 7E shows, the *Gsc* expression domain was maintained in *BAenh*$^{-/-}$ mutant embryos.

There are six *Dlx* genes in mice; *Dlx1/Dlx2*, *Dlx7/Dlx3* and *Dlx5/Dlx6* are organized as physically linked pairs (Stock et al., 1996). *Dlx1* and *Dlx2* are involved in development of derivatives of the maxillary primordia (Qiu et al., 1997; Qiu et al., 1995) and *Dlx5* and *Dlx6* have redundant roles in the development of the mandibular primordia (Acampora et al., 1999; Depew et al., 1999; Robledo et al., 2002), whereas the roles of *Dlx3* and *Dlx7* in craniofacial development have not been elucidated. Although expression of *Dlx2* in the second branchial arch and *Dlx3* in the mandibular and second branchial arch are almost undetectable in *EndrA*$^{-/-}$ embryos, we did not observe any changes in *Dlx2* or *Dlx3* expression in *BAenh*$^{-/-}$ mutants compared with wild-type embryos (data not shown). As Fig. 7F and G show, *Dlx5* and *Dlx6* are robustly

expressed in the ventral aspects of the mandibular and second branchial arches of wild-type and homozygous *BAenh* mutants.

Alx3, a homeobox gene related to *Drosophila aristaless*, is expressed in the neural crest-derived ectomesenchyme in the first and second branchial arches (ten Berge et al., 1998). There was no difference in the expression of *Alx3* between the wild-type and the *BAenh*$^{-/-}$ embryos (data not shown).

DISCUSSION

Ventrolateral expression of *dHAND* in branchial arches 1 and 2 is required for development of distal branchial arch structures

To investigate the role of *dHAND* in development of branchial arch-derived structures, and to determine whether the ETA-dependent branchial arch enhancer of *dHAND* is solely responsible for branchial expression of *dHAND* in vivo, we deleted this enhancer from the mouse genome by targeted mutagenesis. Mice homozygous for this enhancer deletion mutation exhibit lethal craniofacial abnormalities.

Interestingly, the craniofacial defects observed in *BAenh*$^{-/-}$ mutants are milder than those in *ET-1*$^{-/-}$ or *EndrA*$^{-/-}$ mice. The primordium of Meckel's cartilage was observed in *BAenh*$^{-/-}$ mutants at E14.5, and all of the bones and cartilages from the mandibular and hyoid arches were present, though truncated or malformed, indicating that ventrolateral expression of *dHAND* is not required for specification of the cell lineages that contribute to these structures. Rather, dHAND may be involved in differentiation events in these cell lineages such as regulating the genes required for proper condensation and differentiation of cartilages, namely *Bmp2*, *Bmp4* and *Fgf2* (Sarkar et al., 2001). Alternatively, maintenance of *dHAND* expression may be required for continuous proliferation of mesenchymal cells or maintenance of a local concentration of a survival factor such as FGF8 (Schneider et al., 2001), as suggested in the branchial arches of *dHAND* null embryos (Thomas et al., 1998).

It is interesting to note that dHAND has also been shown to regulate patterning of zeugopods and digits of the limbs (Charité et al., 2000). Misexpression of dHAND in the anterior region of the limb bud results in preaxial polydactyly and repatterning of posterior skeletal elements. Conversely, forced expression of dHAND mutant proteins that fail to bind DNA or activate transcription results in truncation of the zeugopods (McFadden et al., 2002). The limb patterning activity of dHAND has been attributed to its ability to induce ectopic expression of sonic hedgehog (Charité et al., 2000), a morphogen that establishes anteroposterior polarity in the developing limbs (Laufer et al., 1994). However, the downstream effectors of dHAND activity in zeugopod outgrowth have not been identified. It is not unreasonable to speculate that the same sets of effector genes might mediate the activity of dHAND in the growth of craniofacial and limb skeletal structures.

Msx1 was previously shown to be down-regulated in branchial arch 1 of *dHAND* null embryos (Thomas et al., 1998), whereas *Msx-1* expression was not affected in *EndrA*$^{-/-}$ null embryos (D. E. C., unpublished observation). In our *BAenh*$^{-/-}$ homozygous mutants, we did not observe a significant change in *Msx1* expression in the area where *dHAND* expression was abolished. This finding could be explained if the remaining ventral (distal) expression of *dHAND* induced a soluble factor(s) to maintain expression of *Msx1* in adjacent cells within the branchial arches. Loss-of-function and gain-of-function of *Msx2* have been reported to cause various craniofacial disorders in humans and mice, suggesting that gene dosage of *Msx2* influences chondrogenesis and osteogenesis in vivo (Liu et al., 1995; Satokata et al., 2000; Wilkie et al., 2000). In the developing mandibular process, BMP4 induces expression of Sox9 and Msx2, which function as positive and a negative regulators of chondrogenesis, respectively (Semba et al., 2000). While the possibility that dHAND is involved in BMP4 signaling in the developing branchial arches remains to be investigated, it is interesting to note that BMP4 is sufficient to induce *dHAND* expression in post-migratory neural crest cells during terminal differentiation to become sympathetic neurons (Howard et al., 2000).

A Dlx6-dependent enhancer controls *dHAND* expression in the ventrolateral, but not distal, portions of branchial arches 1 and 2

Mice homozygous for the deleted enhancer failed to express *dHAND* in the ventrolateral portion of branchial arches 1 and 2. However, *dHAND* expression in the ventral (distal) portion was unaffected in the mutants. Since *dHAND* expression is abolished throughout the branchial arches except in the ventral most tip in *ET-1* and *EndrA*$^{-/-}$ mutant mice, these results strongly suggest the involvement of at least two distinct ETA-dependent enhancers in the control of *dHAND* expression in developing branchial arches 1 and 2 in vivo.

Mesenchymal cells in the dorsal and ventral (distal) regions of the anterior branchial arches appear to be independently specified (Miller et al., 2000). Mosaic analysis in zebrafish showed that ventral postmigratory neural crest cells adopt a ventral fate when they interact with ventral paraxial mesoderm, which expresses *suc*/*ET-1*. These ventral mesenchymal cells were shown to express *dHAND*, *msxE*, *Dlx3* and *EphA3* in a *suc*/*ET-1* dependent manner (Miller et al., 2000). The complexity of *dHAND* expression revealed in the present study clearly points to the involvement of multiple spatially restricted neural crest enhancers in the control *dHAND* expression. Once the distal branchial arch enhancer for *dHAND* is identified, it will be interesting to determine if it shares sequence homology with enhancers that regulate distal arch expression of other genes such as *Msx1* and *eHAND*.

Our results have led us to define two distinct ET-1/ETA-dependent *dHAND* sub-domains in the anterior branchial arches. One is a *Dlx6*-dependent ventrolateral domain controlled by a 208 bp proximal branchial arch enhancer. This *dHAND* expression domain overlaps with the ventrolateral portion of the *Dlx6* expression domain, which depends on ETA-mediated signals (Charité et al., 2001). The other is a ventral domain controlled by a putative distal *dHAND* branchial arch enhancer(s). A recent finding that the expression of *dHAND* is abolished in the branchial arches of *Dlx5/Dlx6* double mutant embryos, which exhibit homeotic transformation of the lower jaw into an upper jaw, suggests that the ventral domain of *dHAND*-expressing cells is controlled by a putative enhancer that is potentially regulated by the combination of these two genes (Beverdam, 2002; Depew, 2002). It is plausible that the loss of both *Dlx5* and *Dlx6* in mandibular arch mesenchyme may affect epithelial expression of soluble factors critical for branchial arch development such

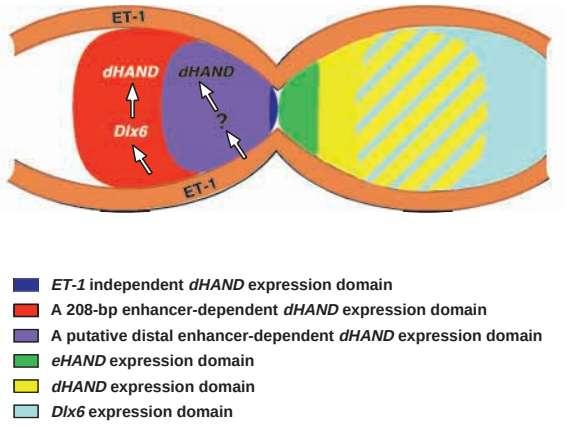

Fig. 8. A model for the regulation of *dHAND* expression during craniofacial development. The expression domains of *dHAND*, *eHAND* and *Dlx6* in the mandibular branchial arch of an E10.5 embryo are shown on the right side. Subdomains of *dHAND* expression are shown on the left side. ET-1 is secreted from the surface epithelium of the branchial arch (shown in brown) and acts on a 208 bp *dHAND* enhancer to induce a ventrolateral domain of *dHAND* (shown in red). The ventral domain of *dHAND* (shown purple) is regulated by unknown branchial arch enchancer(s) via a transcription factor (shown as a question mark) in response to ET-1. The most ventral tip of *dHAND* expression is regulated in an ET-1-independent manner (shown in dark blue).

as BMP7 (Depew, 2002) and ET-1. A third sub-domain of *dHAND* seems to exist in the most ventral region of the branchial arch, which is independent of ET-1/ETA-mediated signals (Fig. 8). Examination of *dHAND* expression in *Dlx6* null embryos may further define *dHAND* sub-domains required for development of the anterior branchial arches.

Multiple and parallel signaling pathways involved in craniofacial development

Craniofacial development is a complex process regulated by a plethora of transcription factors and signaling molecules that comprise multiple independent signaling pathways (Francis-West et al., 1998). One molecule that appears to initiate or maintain one or more of these pathways is ETA, expressed by migratory and post-migratory neural crest cells and their derivatives. We have previously shown that the expression of at least several transcription factors involved in facial patterning is disrupted in *EndrA*$^{-/-}$ mutant embryos. Among those transcription factors, the interrelationship of ETA signaling and *Distalless* function appears to be tightly linked. The expression of *Dlx3*, *Dlx5* and *Dlx6* are all partially or completely disrupted in the *EndrA*$^{-/-}$ mutant embryos, while *Dlx1* and *Dlx2* are largely unaffected. This suggests that ETA signaling is required in a similar manner by linked pairs of *Dlx* genes. Interestingly, disruption of *Dlx5* expression in ETA mutant embryos is only observed in the proximal domains, similar to the pattern observed for *Dlx6* (D. E. C., unpublished observation). However, *Dlx5* and *Dlx6* are likely to be involved in different signaling pathways in facial morphogenesis, as Dlx5 induces *Gsc* expression, while Dlx6 induces *dHAND* expression. Mice homozygous for both *Dlx5* and *Dlx6* develop craniofacial and ear defects, including the failure of Meckel's cartilage, mandible, and calvaria formation, all of which are more severe than those observed in *Dlx5* mutant mice or *EndrA*$^{-/-}$ mutant mice (Robledo et al., 2002). These findings clearly illustrate the similar but non- redundant roles of *Dlx* genes in facial morphogenesis.

dHAND and its branchial arch enhancer as potential targets for mutations in cleft palate syndromes

Cleft palate has a multifactorial etiology and has been associated with abnormal expression of numerous signaling molecules and transcription factors (Ferguson, 1994). Palate formation involves a complex series of steps that include growth of the palatal shelves, palatal elevation and fusion, and disappearance of the midline epithelial seam (Ferguson, 1988). The role of dHAND in the formation of palatine shelves may not be mediated by a direct effect on palatine bone formation. Rather, dHAND may be required for the elevation of the palatine shelves by sustaining concurrent growth of the mandibular bone, as *dHAND*-positive cells do not populate the palatine bones as judged from lineage analysis using *dHAND-Cre*; *R26R* indicator mice (Clouthier et al., unpublished observation). This hypothesis is supported by the observation that a relationship between growth retardation of Meckel's cartilage coupled with relative macroglossia and malformation of the secondary palate is a critical determinant in the development of cleft palate in mice homozygous for a semi-dominant *Col2a1* mutation (Ricks, 2002).

The T-box gene *TBX 22* has been reported to be responsible for CPX (X-linked cleft palate and tongue-tie) syndrome (Braybrook et al., 2001), and a significant linkage-disequilibrium has been found between non-syndromatic cleft lip with or without cleft palate (CL/P) and the *Msx1* and *TGFβ3* genes, and between Cleft Palate Only (CPO) and *Msx1* (Lidral et al., 1998). In addition, craniofacial defects often accompany congenital heart defects as seen in the DiGeorge and Holt-Oram syndromes (Murray, 2001). The expression of *dHAND* during craniofacial as well as cardiovascular development suggests that mutations in the 5′ regulatory region of the *dHAND* gene could also be associated with cleft palate.

We thank Yin Chai Chea for blastocyst injections, J. L. Rubenstein for the Dlx5 probe, Giovanni Levi for the Dlx6 probe, Jeff Stark for histology, Seiji Yokoyama for technical assistance and Alisha Tizenor for graphics. D. E. C. is a recipient of a Career Development Award from the NIDCR/NIH (DE14675). This work was supported by grants from the National Institutes of Health (D. E. C., E. N. O.) and the Donald W. Reynolds Cardiovascular Clinical Research Center, Dallas, Texas to E. N. O.

REFERENCES

Acampora, D., Merlo, G. R., Paleari, L., Zerega, B., Postiglione, M. P. et al. (1999). Craniofacial, vestibular and bone defects in mice lacking the Distal-less-related gene *Dlx*5. *Development* **126**, 3795-3809.

Beverdam, A., Merlo, G. R., Paleari, L., Mantero, S., Genova, F., Barbieri, O., Janvier, P. and Levi, G. (2002). Jaw transformation with gain of symmetry after Dlx5/Dlx6 inactivation: Mirror of the past? *Genesis* **34**, 221-227.

Bouvier, G., Watrin, F., Naspetti, M., Verthuy, C., Naquet, P. and Ferrier, P. (1996). Deletion of the mouse T-cell receptor beta gene enhancer blocks alphabeta T-cell development. *Proc. Natl. Acad. Sci. USA* **93**, 7877-7881.

Braybrook, C., Doudney, K., Marcano, A. C., Arnason, A., Bjornsson, A. et al. (2001). The T-box transcription factor gene TBX22 is mutated in X-linked cleft palate and ankyloglossia. *Nat. Genet.* **29**, 179-183.

Charité, J., McFadden, D. G. and Olson, E. N. (2000). The bHLH transcription factor dHAND controls Sonic hedgehog expression and establishment of the zone of polarizing activity during limb development. *Development* **127**, 2461-2470.

Charité, J., McFadden, D. G., Merlo, G., Levi, G., Clouthier, D. E. et al. (2001). Role of Dlx6 in regulation of an endothelin-1-dependent, dHAND branchial arch enhancer. *Genes Dev.* **15**, 3039-3049.

Clouthier, D. E., Hosoda, K., Richardson, J. A., Williams, S. C., Yanagisawa, H. et al. (1998). Cranial and cardiac neural crest defects in endothelin-A receptor- deficient mice. *Development* **125**, 813-824.

Clouthier, D. E., Williams, S. C., Yanagisawa, H., Wieduwilt, M., Richardson, J. A. and Yanagisawa, M. (2000). Signaling pathways crucial for craniofacial development revealed by endothelin-A receptor-deficient mice. *Dev. Biol.* **217**, 10-24.

Danielian, P. S., Echelard, Y., Vassileva, G. and McMahon, A. P. (1997). A 5.5-kb enhancer is both necessary and sufficient for regulation of Wnt-1 transcription in vivo. *Dev. Biol.* **192**, 300-309.

Depew, M. J., Liu, J. K., Long, J. E., Presley, R. Meneses, J. J. et al. (1999). Dlx5 regulates regional development of the branchial arches and sensory capsules. *Development* **126**, 3831-3846.

Depew, M. J., Lufkin, T. and Rubenstein, J. L. R. (2002). Specification of jaw subdivisions by *Dlx* genes. *Science* **298**, 381-385.

Ferguson, M. W. (1988). Palate development. *Development* **103**, 41-60.

Ferguson, M. W. (1994). Craniofacial malformations: towards a molecular understanding. *Nat. Genet.* **6**, 329-330.

Francis-West, P., Ladher, R., Barlow, A. and Graveson, A. (1998). Signalling interactions during facial development. *Mech. Dev.* **75**, 3-28.

Howard, M. J., Stanke, M., Schneider, C., Wu, X. and Rohrer, H. (2000). The transcription factor dHAND is a downstream effector of BMPs in sympathetic neuron specification. *Development* **127**, 4073-4081.

Jegalian, B. G. and de Robertis, E. M. (1992). Homeotic transformations in the mouse induced by overexpression of a human Hox3.3 transgene. *Cell* **71**, 901-910.

Kempf, H., Linares, C., Corvol, P. and Gasc, J. M. (1998). Pharmacological inactivation of the endothelin type A receptor in the early chick embryo, a model of mispatterning of the branchial arch derivatives. *Development* **125**, 4931-4941.

Kurihara, Y., Kurihara, H., Suzuki, H., Kodama, T., Maemura, K. et al. (1994). Elevated blood pressure and craniofacial abnormalities in mice deficient in endothelin-1. *Nature* **368**, 703-710.

Kurihara, Y., Kurihara, H., Oda, H., Maemura, K., Nagai, R. et al. (1995). Aortic arch malformations and ventricular septal defect in mice deficient in endothelin-1. *J. Clin. Invest.* **96**, 293-300.

Laufer, E., Nelson, C. E., Johnson, R. L., Morgan, B. A. and Tabin, C. (1994). Sonic hedgehog and Fgf-4 act through a signaling cascade and feedback loop to integrate growth and patterning of the developing limb bud. *Cell* **79**, 993-1003.

Le Douarin, N. (1982). *The Neural Crest.* Cambridge, UK: Cambridge University Press.

Lidral, A. C., Romitti, P. A., Basart, A. M., Doetschman, T., Leysens, N. J. et al. (1998). Association of MSX1 and TGFB3 with nonsyndromic clefting in humans. *Am. J. Hum. Genet.* **63**, 557-568.

Liu, Y. H., Kundu, R., Wu, L., Luo, W., Ignelzi, M. A., Jr et al. (1995). Premature suture closure and ectopic cranial bone in mice expressing Msx2 transgenes in the developing skull. *Proc. Natl. Acad. Sci. USA* **92**, 6137-6141.

Liu, J. K., Ghattas, I., Liu, S., Chen, S. and Rubenstein, J. L. (1997). Dlx genes encode DNA-binding proteins that are expressed in an overlapping and sequential pattern during basal ganglia differentiation. *Dev. Dyn.* **210**, 498-512.

Lumsden, A., Sprawson, N. and Graham, A. (1991). Segmental origin and migration of neural crest cells in the hindbrain region of the chick embryo. *Development* **113**, 1281-1291.

Maschhoff, K. L. and Baldwin, H. S. (2000). Molecular determinants of neural crest migration. *Am. J. Med. Genet.* **97**, 280-288.

McFadden, D. G., McAnally, J., Richardson, J. A., Charite, J. and Olson, E. N. (2002). Misexpression of dHAND induces ectopic digits in the developing limb bud in the absence of direct DNA binding. *Development* **129**, 3077-3087.

Miller, C. T., Schilling, T. F., Lee, K., Parker, J. and Kimmel, C. B. (2000). *Sucker* encodes a zebrafish Endothelin-1 required for ventral pharyngeal arch development. *Development* **127**, 3815-3828.

Murray, J. C. (2001). Time for T. *Nat. Genet.* **29**, 107-109.

Noden, D. M. (1988). Interactions and fates of avian craniofacial mesenchyme. *Development* **103**, 121-140.

Qiu, M., Bulfone, A., Martinez, S., Meneses, J. J., Shimamura, K. et al. (1995). Null mutation of Dlx-2 results in abnormal morphogenesis of proximal first and second branchial arch derivatives and abnormal differentiation in the forebrain. *Genes Dev.* **9**, 2523-2538.

Qiu, M., Bulfone, A., Ghattas, I., Meneses, J. J., Christensen, L. et al. (1997). Role of the Dlx homeobox genes in proximodistal patterning of the branchial arches, mutations of Dlx-1, Dlx-2, and Dlx-1 and –2 alter morphogenesis of proximal skeletal and soft tissue structures derived from the first and second arches. *Dev. Biol.* **185**, 165-184.

Ricks, J. E., Ryder, V. M., Bridgewater, L. C., Schaalje, B. and Seegmiller, R. E. (2002). Altered mandibular development precedes the time of palate closure in mice homozygous for disproportionate micromelia, An oral clefting model supporting the Pierre-Robin sequence. *Teratology* **65**, 116-120.

Robledo, R. F., Rajan, L., Li, X. and Lufkin, T. (2002). The Dlx5 and Dlx6 homeobox genes are essential for craniofacial, axial, and appendicular skeletal development. *Genes Dev.* **16**, 1089-1101.

Sakai, K. and Miyazaki, J. (1997). A transgenic mouse line that retains Cre recombinase activity in mature oocytes irrespective of the cre transgene transmission. *Biochem. Biophys. Res. Commun.* **237**, 318-324.

Sarkar, S., Petiot, A., Copp, A., Ferretti, P. and Thorogood, P. (2001). FGF2 promotes skeletogenic differentiation of cranial neural crest cells. *Development* **128**, 2143-2152.

Satokata, I. and Maas, R. (1994). Msx1 deficient mice exhibit cleft palate and abnormalities of craniofacial and tooth development. *Nat Genet* **6**, 348-356.

Satokata, I., Ma, L., Ohshima, H., Bei, M., Woo, I. et al. (2000). Msx2 deficiency in mice causes pleiotropic defects in bone growth and ectodermal organ formation. *Nat. Genet.* **24**, 391-395.

Schneider, R. A., Hu, D., Rubenstein, J. L., Maden, M. and Helms, J. A. (2001). Local retinoid signaling coordinates forebrain and facial morphogenesis by maintaining FGF8 and SHH. *Development* **128**, 2755-2767.

Semba, I., Nonaka, K., Takahashi, I., Takahashi, K., Dashner, R. et al. (2000). Positionally-dependent chondrogenesis induced by BMP4 is co-regulated by Sox9 and Msx2. *Dev. Dyn.* **217**, 401-414.

Shelton, J. M., Lee, M. H., Richardson, J. A. and Patel, S. B. (2000). Microsomal triglyceride transfer protein expression during mouse development. *J. Lipid Res.* **41,** 533-537.

Srivastava, D., Thomas, T., Lin, Q., Kirby, M. L., Brown, D. and Olson, E. N. (1997). Regulation of cardiac mesodermal and neural crest development by the bHLH transcription factor, dHAND. *Nat. Genet.* **16**, 154-160.

Stock, D. W., Ellies, D. L., Zhao, Z., Ekker, M., Ruddle, F. H. and Weiss, K. M. (1996). The evolution of the vertebrate Dlx gene family. *Proc. Natl. Acad. Sci. USA* **93**, 10858-10863.

Takahashi, K., Nuckolls, G. H., Takahashi, I., Nonaka, K., Nagata, M. et al. (2001). Msx2 is a repressor of chondrogenic differentiation in migratory cranial neural crest cells. *Dev. Dyn.* **222**, 252-262.

ten Berge, D., Brouwer, A., el Bahi, S., Guenet, J. L., Robert, B. and Meijlink, F. (1998). Mouse Alx3, an aristaless-like homeobox gene expressed during embryogenesis in ectomesenchyme and lateral plate mesoderm. *Dev. Biol.* **199**, 11-25.

Thomas, T., Kurihara, H., Yamagishi, H., Kurihara, Y., Yazaki, Y. et al. (1998). A signaling cascade involving endothelin-1, dHAND and msx1 regulates development of neural-crest-derived branchial arch mesenchyme. *Development* **125**, 3005-3014.

Trainor, P. A., Ariza-McNaughton, L. and Krumlauf, R. (2002). Role of the isthmus and FGFs in resolving the paradox of neural crest plasticity and prepatterning. *Science* **295**, 1288-1291.

Wilkie, A. O., Tang, Z., Elanko, N., Walsh, S., Twigg, S. R. et al. (2000). Functional haploinsufficiency of the human homeobox gene MSX2 causes defects in skull ossification. *Nat. Genet.* **24**, 387-390.

Yamada, G., Mansouri, A., Torres, M., Stuart, E. T. and Blum, M. et al. (1995). Targeted mutation of the murine goosecoid gene results in craniofacial defects and neonatal death. *Development* **121**, 2917-2922.

Yanagisawa, H., Yanagisawa, M., Kapur, R. P., Richardson, J. A., Williams, S. C. et al. (1998). Dual genetic pathways of endothelin-mediated intercellular signaling revealed by targeted disruption of endothelin converting enzyme-1 gene. *Development* **125**, 825-836.

Yanagisawa, H., Hammer, R. E., Richardson, J. A., Emoto, N., Williams, S. C. et al. (2000). Disruption of ECE-1 and ECE-2 reveals a role for endothelin-converting enzyme-2 in murine cardiac development. *J. Clin. Invest.* **105**, 1373-1382.